

Four-Wave mixing in degenerate Fermi gases: Beyond the undepleted pump approximation

T. Miyakawa,^{1,2} H. Christ,¹ C. P. Search,¹ and P. Meystre¹

¹*Optical Sciences Center, The University of Arizona, Tucson, AZ 85721*

²*Department of Physics, Tokyo Metropolitan University,
1-1 Minami-Ohsawa, Hachioji, Tokyo 192-0397, Japan*

(Dated: October 29, 2018)

We analyze the full nonlinear dynamics of the four-wave mixing between an incident beam of fermions and a fermionic density grating. We find that when the number of atoms in the beam is comparable to the number of atoms forming the grating, the dephasing of that grating, which normally leads to a decay of its amplitude, is suppressed. Instead, the density grating and the beam density exhibit large nonlinear coupled amplitude oscillations. In this case four-wave mixing can persist for much longer times compared to the case of negligible back-action. We also evaluate the efficiency of the four-wave mixing and show that it can be enhanced by producing an initial density grating with an amplitude that is less than the maximum value. These results indicate that efficient four-wave mixing in fermionic alkali gases should be experimentally observable.

PACS numbers: 03.75.Fi, 05.30.Fk

INTRODUCTION

In recent years the field of nonlinear atom optics [1] has become firmly established both theoretically and experimentally with the demonstration of four-wave mixing in Bose-Einstein condensates [2], coherent matter wave amplification [3], the creation of dark [4] and bright [5] atomic solitons, the generation of correlated atomic pairs and squeezing [6, 7], and the creation of a molecular condensate – the analog of second-harmonic generation in optics [8, 9]. So far, this work has been largely limited to bosonic atoms and has been based to a great extent on analogies with nonlinear optics: Ultracold bosons interact primarily via s -wave collisions and typically occupy only a few quantum states, so that their mean-field description in terms of a Gross-Pitaevskii equation includes a nonlinearity of the same form as a third-order optical Kerr nonlinearity, and thus many of the results from nonlinear optics can be directly applied to condensates. In particular, Bose-Einstein condensates are often viewed as a matter-wave equivalent of the optical laser – the so called "atom laser".

The last few years have also seen substantial progress in the cooling and trapping of atomic Fermi gases to the quantum degenerate regime, with temperatures reaching as low as $T < 0.2T_F$ where T_F is the Fermi temperature [10, 11, 12, 13, 14]. It is therefore only a matter of time before experiments start to probe the dynamics of these gases far from equilibrium and perform fermionic nonlinear atom optics experiments. However, the extension of the ideas developed in nonlinear optics to Fermi systems is by no means obvious or straightforward because of the different quantum statistics obeyed by fermions and bosons. Whereas for bosons the analysis can typically be limited to a few macroscopically occupied modes, the Pauli exclusion principle prohibits

the number of modes from ever being less than the number of particles for fermions. This makes both analytical and numerical studies of the dynamics of Fermi systems rather challenging, except for very limited situations (e.g. $T = 0$ and weak perturbations). Consequently, the idea of doing nonlinear atom optics with fermions is still new and largely unexplored.

It is only recently that it has been convincingly argued that four-wave mixing is possible with fermions [15, 16]. These works showed how four-wave mixing can be interpreted in terms of incident particles undergoing Bragg scattering off of a fermionic density grating, but were limited to an incident beam consisting of a single test particle. They also neglected the dynamics of the density grating. Related work has shown that four-wave mixing between a degenerate fermion beam and a bosonic density grating is also possible [17]. While these results are promising, a complete analysis of purely fermionic four-wave mixing is still lacking.

In a previous paper [18], we studied fermionic four-wave mixing using the matter-wave analog of the undepleted pump approximation in optics, i.e. we neglected the back-action of the diffracted atoms on the density grating. The density grating was formed by atoms in a single hyperfine state prepared in a coherent superposition of the momentum states $k - q/2$ and $k + q/2$ for all k such that $|k| < k_{F,g}$, where $k_{F,g}$ is the Fermi wave number of the grating atoms and q the wave number of the density modulation. The third incident wave consisted of a degenerate Fermi gas in a different hyperfine state so that the atoms in the beam and grating could interact via s -wave collisions. These atoms could then be diffracted by the density grating to produce a fourth, scattered wave. Because of the range of energy states occupied by its constituent atoms, the amplitude of the grating would decay away due to the dephasing of the

atoms. This led to a finite time during which four-wave mixing could occur and placed serious constraints on the properties of the fermions involved.

In this paper, we extend the results of Ref. [18] by taking into account the back-action of the incident beam on the fermionic density grating. We find that when the number of atoms in the incident beam becomes a sizable fraction of the number of atoms forming the density grating, it no longer decays away due to the dephasing. Instead, it exhibits large nonlinear amplitude oscillations that are coupled to the Bragg oscillations of the beam. This leads to the efficient generation of the fourth scattered wave, even for times much longer than the grating dephasing time. We interpret this behavior in terms of a Bloch vector picture. We also evaluate the efficiency for the generation of the scattered wave and show that it should be possible to produce a macroscopic fourth wave. Interestingly enough, we find that the efficiency of the four-wave mixing can be improved significantly by initially preparing a density grating with an amplitude that is less than maximal.

The organization of this paper is as follows: In section II, we briefly review the model developed in [18]. Section III presents numerical results that show how the dephasing of the grating can be eliminated when the back-action becomes significant. The efficiency of the four-wave mixing is also calculated and it is shown that a macroscopic fourth wave can be readily produced. Finally, section IV is a summary and conclusion. The appendix presents an analytically soluble model in terms of coupled Bloch vectors that yields a qualitative interpretation of our results.

MODEL

In this section we briefly review the one-dimensional model developed in [18] to study four-wave mixing between fermions at zero temperature. We consider two spin-polarized species of fermions— a density grating composed of spin-up polarized atoms and an incident beam of spin-down polarized atoms, see Fig. 1. Atoms in different spin states interact via elastic s -wave scattering. The cross-section for p -wave scattering at $T = 0$ is orders of magnitude smaller than that of s -wave scattering, thus p -wave scattering is neglected in our model [19].

For clarity and simplicity we restrict ourselves to one spatial dimension. It is usually possible to reduce the problem of four-wave mixing to a two-dimensional planar geometry, with one dimension parallel to the density grating. Since the momentum transfer to the beam atoms is parallel to the density modulation of the grating, the essential dynamics of the wave mixing process occurs only in that \hat{z} -direction. We assume that the grating is confined between $x = 0$ to $x = d$ along the perpendicular \hat{x} axis. If the average momentum, $\hbar k_{\perp}$, of the atomic beam along that direction is sufficiently large

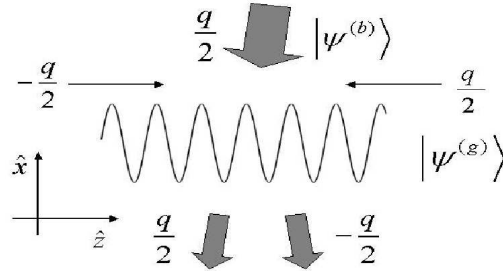


FIG. 1: Model of the scattering. The spin-down polarized beam is scattered (s -wave) by a spin-up polarized grating.

that $k_{\perp} \gg 1/d$, then the requirements of energy and momentum conservation insure that k_{\perp} remains practically unchanged by the scattering. In this case, wave mixing in two or three dimensions is in essence the same as in the one-dimensional model that we consider. (The transverse momenta of the beam atoms can at most change sign due to reflection off the grating at $x = 0$ [17], but the reflected wave can be minimized by using a smooth grating density profile in the \hat{x} -direction.)

The second quantized Hamiltonian describing the situation at hand is

$$H = \sum_k \hbar \omega_k \left(a_{k\uparrow}^{\dagger} a_{k\uparrow} + a_{k\downarrow}^{\dagger} a_{k\downarrow} \right) + \hbar U_0 \sum_{k_1, k_2, q} \left(a_{k_1+q\uparrow}^{\dagger} a_{k_2-q\downarrow}^{\dagger} a_{k_2\downarrow} a_{k_1\uparrow} \right), \quad (1)$$

with $\omega_k = \hbar k^2/2m$ and $U_0 = 4\pi\hbar a/(Ld^2m)$. Here, a is the scattering length, d^2 is the transverse cross-sectional area, m the mass of one atom and L the quantization length. The operators $a_{k,\sigma}$ and $a_{k,\sigma}^{\dagger}$ are annihilation and creation operators for atoms with momentum $\hbar k$ and spin $\sigma = \uparrow, \downarrow$, satisfying standard fermionic anticommutation relations.

The dynamics of the system is conveniently described in terms of the particle-hole operators

$$\begin{aligned} \rho_{k,k'}^{(b)} &= a_{k+k'\downarrow}^{\dagger} a_{k\downarrow}, \\ \rho_{k,k'}^{(g)} &= a_{k+k'\uparrow}^{\dagger} a_{k\uparrow}, \end{aligned} \quad (2)$$

that create a particle in state $k + k'$ and a hole in k for the beam and grating, respectively. They obey the Heisenberg equations of motion

$$\begin{aligned} i \frac{d}{dt} \rho_{k,k'}^{(b,g)} &= \omega_{k,k'} \rho_{k,k'}^{(b,g)} \\ &+ U_0 \sum_{k_1, k_2} \left(\rho_{k+k_1, k'-k_1}^{(b,g)} - \rho_{k,k'-k_1}^{(b,g)} \right) \rho_{k_2, k_1}^{(g,b)}, \end{aligned} \quad (3)$$

with $\omega_{k,k'} = \omega_k - \omega_{k+k'}$.

We consider a beam of N_b atoms propagating along the \hat{x} -direction, but with a small momentum component around a central value \bar{q} parallel to the grating, which is taken to be in a superposition of the states $k - q/2$ and $k + q/2$ for $-k_{F,g} \leq k \leq k_{F,g}$. Here, $k_{F,g} = \pi N_g/L$ is the Fermi momentum (in one dimension) and N_g is the number of atoms in the grating. Such a grating can be created from a stationary homogeneous gas by a two-step process where first a two-photon Bragg π -pulse imparts a momentum $-\hbar q/2$ to each atom, followed by a second Bragg pulse with momentum $\hbar q$ that creates the desired superposition (see e.g. Ref. [20]). (Note that the bandwidth of the pulses should be greater than $\omega_{k_{F,g}}$.) Thus the initial state of the beam-grating system is

$$|\Psi(0)\rangle = |\Psi^{(b)}\rangle |\Psi^{(g)}\rangle, \quad (4)$$

where

$$\begin{aligned} |\Psi^{(g)}\rangle &= \prod_{|k| \leq k_{F,g}} \frac{1}{\sqrt{2}} \left(a_{k-q/2\uparrow}^\dagger + a_{k+q/2\uparrow}^\dagger \right) |0\rangle, \\ |\Psi^{(b)}\rangle &= \prod_{|k| \leq k_{F,b}} a_{k+\bar{q}\downarrow}^\dagger |0\rangle. \end{aligned} \quad (5)$$

$k_{F,b} = \pi N_b/L$ being the Fermi momentum of the beam.

The initial expectation values of the particle-hole operators $\rho_{k,k'}^{(b)}$ and $\rho_{k,k'}^{(g)}$ are readily found to be

$$\begin{aligned} \langle \Psi^{(b)} | \rho_{k,k'}^{(b)}(0) | \Psi^{(b)} \rangle &= \delta_{k',0} \Theta(k_{F,b} - |k - \bar{q}|), \\ \langle \Psi^{(g)} | \rho_{k,k'}^{(g)}(0) | \Psi^{(g)} \rangle &= \frac{1}{2} (\delta_{k',0} + \delta_{k',q}) \Theta(k_{F,g} - |k + \frac{q}{2}|) \\ &\quad + \frac{1}{2} (\delta_{k',0} + \delta_{k',-q}) \Theta(k_{F,g} - |k - \frac{q}{2}|). \end{aligned} \quad (6)$$

We note that the spatial density of the Fermi gas is given by

$$\rho^{(b,g)}(x) = \frac{1}{L} \sum_{k'} \left(\sum_k \langle \rho_{k,k'}^{(b,g)} \rangle \right) e^{-ik'x}, \quad (7)$$

from which it is clear that the density for the initial state of the spin-up polarized grating atoms exhibits as expected a spatial modulation with the grating wave number q and an amplitude N_g/L . In contrast, the spin-down polarized incident beam has a uniform density.

It is convenient to introduce the slowly varying particle-hole operators $\rho_{k,k'}^{(b,g)}(t) = \hat{\rho}_{k,k'}^{(b,g)}(t) e^{-i\omega_{k,k'}t}$ whose Heisenberg equation of motion simply become

$$\frac{d}{dt} \hat{\rho}_{k,k'}^{(b,g)} = -iU_0 \sum_{k_1,k_2} \left(\hat{\rho}_{k+k_1,k'-k_1}^{(b,g)} e^{i(\omega_{k,k_1} - \omega_{k_2,k_1})t} - \hat{\rho}_{k,k'-k_1}^{(b,g)} e^{-i(\omega_{k+k',-k_1} + \omega_{k_2,k_1})t} \right) \hat{\rho}_{k_2,k_1}^{(g,b)}(t), \quad (8)$$

In the following we factorize the expectation values of these operators for different spin states,

$$\langle \hat{\rho}_{k,q}^{(g)} \hat{\rho}_{k',k''}^{(b)} \rangle \approx \langle \hat{\rho}_{k,q}^{(g)} \rangle \langle \hat{\rho}_{k',k''}^{(b)} \rangle. \quad (9)$$

This ansatz results in the truncation of the BBGKY-type hierarchy of equations of motion for the higher-order moments of the particle-hole operators after the first moments [22], yielding the closed set of c -number equations

$$\frac{d}{dt} \bar{\rho}_{k,k'}^{(b,g)} = -iU_0 \sum_{k_1,k_2} \left(\bar{\rho}_{k+k_1,k'-k_1}^{(b,g)} e^{i(\omega_{k,k_1} - \omega_{k_2,k_1})t} - \bar{\rho}_{k,k'-k_1}^{(b,g)} e^{-i(\omega_{k+k',-k_1} + \omega_{k_2,k_1})t} \right) \bar{\rho}_{k_2,k_1}^{(g,b)}(t), \quad (10)$$

where $\bar{\rho}_{k,k'}^{(g)} \equiv \langle \hat{\rho}_{k,k'}^{(g)} \rangle$ and $\bar{\rho}_{k,k'}^{(b)} \equiv \langle \hat{\rho}_{k,k'}^{(b)} \rangle$. These equations can be readily integrated numerically.

Implicit in Eqs. (10) and (6) are the three fundamental time scales that govern the dynamics of the interaction between the beam and the grating. The first time scale is associated with the kinetic energy ω_q gained by an atom scattered by the grating. The other two time scales are associated with the density grating itself. If, for the moment, we revert to the undepleted pump approximation used in Ref. [18], namely $\bar{\rho}_{k,q}^{(g)}(t) = \bar{\rho}_{k,q}^{(g)}(0)$, then we ob-

tain the linear equations of motion for the beam,

$$\begin{aligned} \frac{d}{dt} \bar{\rho}_{k,k'}^{(b)} &= -ig(t) \left(\bar{\rho}_{k+q,k'-q}^{(b)} e^{i\omega_{k,q}t} - \bar{\rho}_{k,k'-q}^{(b)} e^{-i\omega_{k+k',-q}t} \right. \\ &\quad \left. - \bar{\rho}_{k-q,k'+q}^{(b)} e^{i\omega_{k,-q}t} + \bar{\rho}_{k,k'+q}^{(b)} e^{-i\omega_{k+k',q}t} \right). \end{aligned} \quad (11)$$

Here

$$\begin{aligned} g(t) &= \frac{U_0}{2} \sum_{k_2} \Theta(k_{F,g} - |k_2 + q/2|) e^{-i\omega_{k_2,q}t} \\ &= \frac{U_0 N_g}{2} \text{sinc} \left(\frac{\hbar q k_{F,g} t}{m} \right), \end{aligned}$$

where the second equality was obtained in the continuum limit, $\sum_k \rightarrow L/2\pi \int dk$. The coupling constant $g(t)$ is proportional to the amplitude of the density grating, which decays to zero in a time of the order of

$$\tau_D = m/\hbar q k_{F,g}.$$

This decay is caused by the spread in energies of the fermions that comprise the grating, $\hbar\Delta\omega = \hbar|\omega_{k_{F,g}+q/2} - \omega_{k_{F,g}-q/2}|$, so that the different energy states in the grating get out of phase with each other over time. This leads to an effective grating lifetime of the order of $\tau_D = 1/\Delta\omega$, which corresponds to the relative phases of the different states being of order unity.

The third time scale is given by the characteristic time

$$\tau_B = 1/U_0 N_g$$

for atoms to scatter off of the grating in the limit of a static grating ($\tau_D \rightarrow \infty$). For an incident particle with momentum $\pm q/2$, τ_B^{-1} is the frequency of oscillations between the degenerate states $q/2$ and $-q/2$. In the Bragg regime that we consider in this paper, both the kinetic energy and the momentum of the atoms are conserved by the scattering process. This corresponds to the condition,

$$\omega_q \tau_B \gg 1.$$

The population that develops in states centered around $\pm 3q/2, \pm 5q/2, \dots$ is then at most on the order of $(\tau_B \omega_q)^{-2}$. If we choose the average momentum of the beam as $\bar{q} = q/2$, with $\bar{q} > k_{F,b}$, only states centered around $-q/2$ are phase-matched to the states in the incident beam, so that we can restrict ourselves to those k states within a width $2k_{F,b}$ of $\pm q/2$. (This is in contrast to the Raman-Nath regime, where the change in the kinetic energy of an atom as result of scattering off of the grating is negligible compared to the interaction energy with the grating [21].)

In the undepleted pump approximation it is important that the scattering time be less than the lifetime of the grating,

$$\tau_B < \tau_D, \quad (12)$$

otherwise there is no significant scattering beam generated. However, as we show in the next section, four-wave mixing can continue for times much longer than τ_D when the effects of the back-action on the grating become significant.

NUMERICAL RESULTS

In this section we study the phenomena in fermionic four-wave mixing resulting from the back-action of the atomic beam on the grating. We proceed by numerically

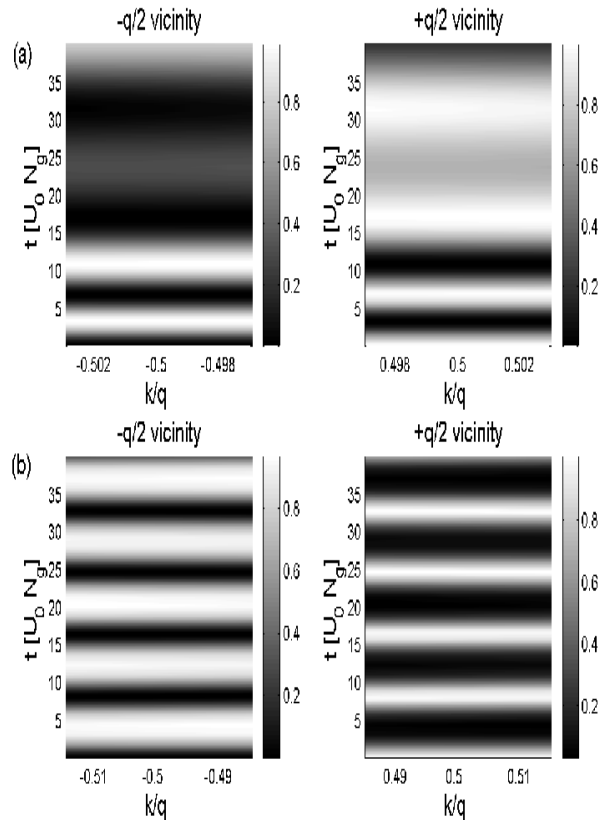


FIG. 2: Populations $n_k^{(b)}$ as a function of time (in units of $\tau_B = 1/U_0 N_g$) for (a) $N_b/N_g = 0.1$ and (b) $N_b/N_g = 0.5$. In both cases $\tau_D/\tau_B = 7.5$ and $\omega_q/(U_0 N_g) = 2$.

solving Eqs. (10), subject to the initial conditions (6) with $\bar{q} = q/2 > k_{F,b}$, using a fourth-order Runge-Kutta algorithm with fixed time steps chosen to produce a relative error smaller than 1%.

The back-action of the beam on the density grating is negligible for all times when the number of beam atoms is much less than the number of atoms in the grating, $N_g \gg N_b$. The reason is that for every atom in the beam that suffers a momentum transfer of $\pm \hbar q$, one atom of the grating sees its wave function “reduced” from the superposition state $(|k - q/2\rangle + |k + q/2\rangle)/\sqrt{2}$ to the state $|k \mp q/2\rangle$. Since only those atoms in a superposition of $k - q/2$ and $k + q/2$ (for all possible k) contribute to the density modulation, the fractional reduction in the amplitude of the grating will be at most $N_b/N_g \ll 1$ and the undepleted pump approximation is valid for all times. This approximation also holds for arbitrary N_b for times short enough that the number of atoms scattered by the grating is much less than N_g , that is, for times $t \ll \tau_B$.

Fermionic four-wave mixing is conveniently characterized in terms of the occupation numbers of the momen-

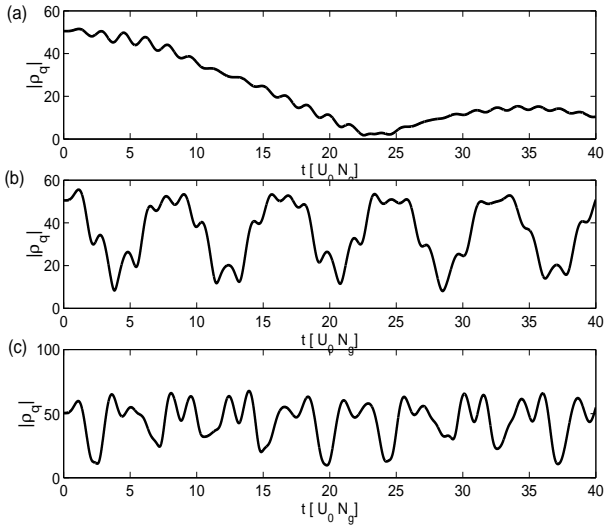


FIG. 3: The densities $|\rho_q|$ as a function of time scaled by $U_0 N_g$ for the ratios $N_b/N_g = 0.1, 0.5$ and 1.0 in the subplot (a), (b) and (c), respectively.

tum states of the beam and grating atoms

$$n_k^{(b,g)}(t) = \bar{\rho}_{k,0}^{(b,g)}(t), \quad (13)$$

and the amplitude of the density modulation of the grating,

$$\rho_q(t) = \sum_k \bar{\rho}_{k,q}^{(g)}(t) e^{-i\omega_{k,q}t}. \quad (14)$$

Fig. 2a plots $n_k^{(b)}$ as a function of time for the case of a “large” grating, $N_b/N_g = 0.1$ and $\tau_D/\tau_B = 7.5$, and Fig. 3a shows the evolution of the density modulation of the grating $|\rho_q(t)|$ for these same parameters. The atoms in the beam undergo Bragg oscillations between the k states centered around $-q/2$ and $+q/2$ up until a time of the order of τ_D , when the amplitude of the oscillations dies out. It is clear from the behavior of $|\rho_q(t)|$ that the disappearance of the Bragg oscillations corresponds to the decay of the grating amplitude due to dephasing. In this example, the back-action of the beam on the grating manifests itself in the small amplitude oscillations superimposed on the sinc function behavior of $|\rho_q(t)|$. These oscillations reflect the coupling between individual modes of the beam and of the grating, which all occur at roughly the same frequency τ_B^{-1} for $\tau_B^{-1} \gg |kq/m|$, as further discussed later on.

Figs. 2b and 4b are the same as Fig. 2a except that “smaller” gratings, with $N_b/N_g = 0.5$ and $N_b/N_g = 1.0$, respectively, have been used. For these parameters there is a dramatic change in the behavior of $|\rho_q(t)|$ as the back-action becomes more pronounced. Instead of decaying away, the density grating now undergoes large amplitude

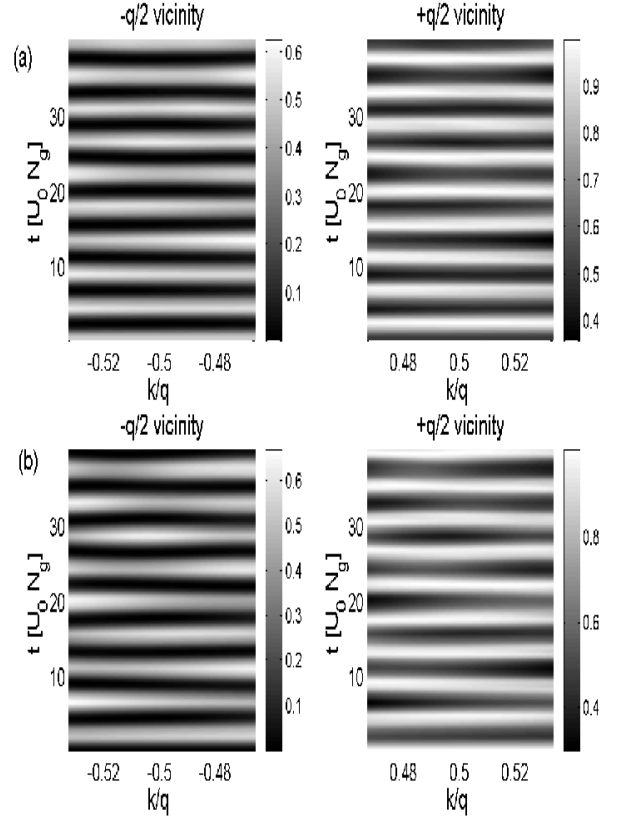


FIG. 4: Atomic populations as a function of time (in units of $\tau_B = 1/U_0 N_g$) for the case of equal particle numbers $N_b/N_g = 1.0$. The upper plots (a) show the density of the grating, $n_k^{(g)}$, and the lower plots (b) show the beam evolution, $n_k^{(b)}$.

oscillations, as illustrated in Fig. 3. At the same time, the beam atoms undergo nearly perfect Bragg oscillations that persist for times much longer than τ_D . Note that the amplitude of the oscillations is equal to 1 for $N_b/N_g = 0.5$, but only to about 1/2 for $N_b/N_g = 1.0$ (see the scales of the grey-scale plots) although there is no evidence of any decay in the Bragg oscillations.

If one ignores the weak population of the states centered around $\pm 3q/2, \pm 5q/2, \dots$ (an approximation valid in the Bragg regime) these coupled oscillations involve the oscillation of a beam atom between the states $|k' + q/2\rangle$ and $|k' - q/2\rangle$, while an atom in the grating oscillates between $|k - q/2\rangle$ and $|k + q/2\rangle$, $\pi/2$ out of phase with the beam atom, as follows from the existence of the constants of motion

$$\sum_{|k| < k_{F,g}} n_{k+q/2}^{(g)} + \sum_{|k| < k_{F,b}} n_{k+q/2}^{(b)}, \quad (15)$$

$$\sum_{|k| < k_{F,g}} n_{k-q/2}^{(g)} + \sum_{|k| < k_{F,b}} n_{k-q/2}^{(b)}. \quad (16)$$

We can gain a better understanding of fermionic four-

wave mixing by recasting it in terms of the dynamics of an inhomogeneously broadened ensemble of coupled two-level systems. In this picture, an individual two-level system consists of the manifold of beam and grating states $\{|k - q/2\rangle, |k + q/2\rangle\}$ for all states with $|k| < k_{F,g}$ and $|k| < k_{F,b}$ for the grating and beam atoms, respectively. We proceed by introducing the associated Bloch vectors [23],

$$\mathbf{U}_k^{(g)} = U_k^{(g)} \hat{\mathbf{x}} + V_k^{(g)} \hat{\mathbf{y}} + W_k^{(g)} \hat{\mathbf{z}}, \quad (17)$$

with the components

$$U_k^{(g)}(t) = \rho_{k-q/2,q}^{(g)}(t) + \rho_{k+q/2,-q}^{(g)}(t), \quad (18)$$

$$V_k^{(g)}(t) = i\rho_{k-q/2,q}^{(g)}(t) - i\rho_{k+q/2,-q}^{(g)}(t), \quad (19)$$

$$W_k^{(g)}(t) = n_{k+q/2}^{(g)} - n_{k-q/2}^{(g)}. \quad (20)$$

It is easily seen that the Bloch vectors associated with the atoms in the incident beam obey the equations of motion

$$\frac{d}{dt} \mathbf{U}_k^{(g)}(t) = \mathbf{U}_k^{(g)}(t) \times \mathbf{R}_k^{(b)}(t), \quad (21)$$

that is, they precess around the effective field

$$\mathbf{R}_k^{(b)}(t) = U_0 \sum_{k'} U_{k'}^{(b)} \hat{\mathbf{x}} + U_0 \sum_{k'} V_{k'}^{(b)} \hat{\mathbf{y}} + \delta\omega_k \hat{\mathbf{z}}, \quad (22)$$

where

$$\delta\omega_k = \frac{\hbar k q}{m}. \quad (23)$$

Here, $U_{k'}^{(b)}$ and $V_{k'}^{(b)}$ are the components of the k' -th Bloch vector for the beam, $\mathbf{U}_{k'}^{(b)}$. They are defined in the same way as Eqs. (17)-(20) for the grating. Clearly, the grating Bloch vector $\mathbf{U}_k^{(b)}$ also obeys Eq. (21), with the interchange $b \leftrightarrow g$.

The components of the Bloch vector in the equatorial ($\hat{x}\hat{y}$) plane of the Bloch sphere are a measure of the coherence between the momentum states $|k - q/2\rangle$ and $|k + q/2\rangle$ and therefore the sum of the projections of the grating Bloch vectors onto the equatorial plane is equal to the amplitude of the density grating.

Initially all of the Bloch vectors for the grating point along the \hat{x} axis, while those of the atomic beam, which doesn't exhibit any coherence, point toward the north pole ($+\hat{z}$) of the Bloch sphere. (That they point north rather than south follows from the fact that the initial momenta of the beam are in an interval of width $k_{F,b}$ about $\bar{q} = q/2$, see Eq. (6). We have seen that the Bragg regime requires additionally that $\bar{q} > k_{F,b}$, so that $n_{k-q/2}^{(b)}$ is initially equal to zero and $W_k^{(b)} > 0$.)

In the absence of any coupling to the beam, $U_0 = 0$, the version of Eq. (21) for the grating shows that the

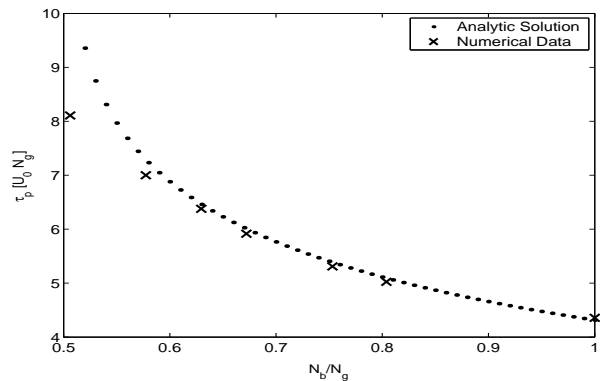


FIG. 5: Crosses: numerically obtained period of oscillation τ_p of the atomic densities; Dotted line: analytic result of Eq. (24). Time in units of $U_0 N_g$.

evolution of the Bloch vectors is simply a rotation in the equatorial plane at frequency $\delta\omega_k$. This “inhomogeneous broadening” causes the grating to dephase because of the spreading out of the Bloch vectors in the equatorial plane.

Consider now the other extreme situation where the collisional coupling between the beam and grating atoms completely dominates the dynamics, i.e. $U_0 N_b \sim U_0 N_g \sim U_0 \sum_k U_k^{(g)}(t) \gg \delta\omega_k$ or equivalently, $\tau_D \gg \tau_B$. The amplitude of the effective field that drives the grating, $U_0 \sum_k V_k^{(b)}(t)$, is initially equal to zero since the initial Bloch vectors of the beam point towards the north pole ($+\hat{z}$) of the Bloch sphere. However, those vectors start rotating around the \hat{x} -axis under the influence of the instantaneous grating effective field $U_0 \sum_k U_k^{(g)}(t)$, leading in turn to a projection along the \hat{y} -axis. This then allows the Bloch vector of the grating to start rotating about that axis towards the north pole of the Bloch sphere at the instantaneous frequency $U_0 \sum_k V_k^{(b)}(t)$. As $\mathbf{U}_k^{(b)}$ approaches the \hat{y} -axis, $\mathbf{U}_k^{(g)}$ reaches the north pole and its projection on the equatorial plane vanishes and then changes sign. This reverses the sense of rotation of the beam Bloch vectors, which begin to move back toward the pole, at which point their projections on the \hat{y} -axis likewise change sign. This reverses the direction of rotation of $\mathbf{U}_k^{(g)}$, which then passes back through the north pole, reversing the sense of rotation of $\mathbf{U}_k^{(b)}$, etc. We see that the beam atoms are transformed into a grating-like superpositions state, and at the same time the atoms forming the initial grating take on a state similar to the initial beam state. Thus, as time passes, the labels “beam” and “grating” become more and more interchangeable. One result of this back-and-forth is that the oscillation frequency of the populations is twice that of the coherences. Furthermore, their amplitude is only 1/2, both for the beam and the grating, since the Bloch vectors are confined to the Northern hemisphere of the

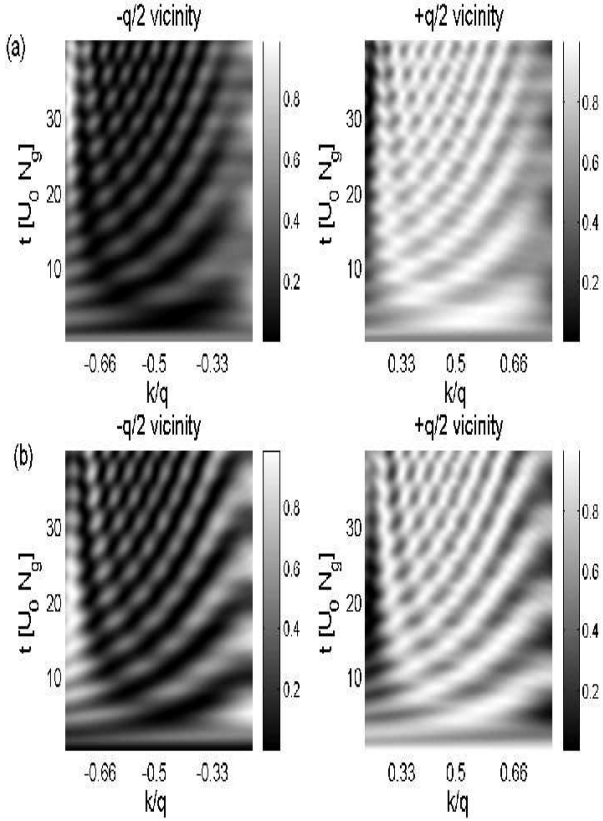


FIG. 6: Atomic populations $n_k^{(b,g)}$ as a function of time (in units of $\tau_B = 1/U_0 N_g$) for the case of short dephasing time $\tau_D/\tau_B = 1.0$, with $N_b/N_g = 1.0$ and $\omega_q/N_g U_0 = 2$. The upper plots are for the grating and the lower plots for the beam.

Bloch sphere, $0 \leq W_k^{(b,g)} \leq 1$. This explains the reduced amplitude of the oscillations in Fig. 4.

The analytic solution of this model given in the appendix yields, for $N_b > N_g/2$, an oscillation period of

$$\tau_p = 2\pi/\Omega_0 = \frac{2}{U_0 \sqrt{N_g N_b}} F((1/2 + N_g/4N_b)^{1/2}, \pi/2), \quad (24)$$

where $F(k, \pi/2)$ is the complete elliptic integral of the first kind [28].

We have numerically calculated the Fourier transform of $n_k^{(b,g)}(t)$ for $k_{F,b}, k_{F,g} \ll q$ and $\tau_D/\tau_B = 2$ and confirmed that the populations of the grating and the beam oscillate at the same frequency Ω_0 independently of k . Fig. (5) compares the period of oscillations τ_p as a function of N_b for fixed N_g to the analytical result of Eq. (24), showing a very good agreement. We find that the dominant frequency in the evolution of $\rho_q(t)$ is approximately $\Omega_0/2$, in agreement with the predictions of Bloch vector model. The small amplitude, high-frequency oscillations in $\rho_q(t)$ are due to a residual coupling to mo-

mentum states around $\pm 3q/2$.

The picture that we have developed indicates that the effects of dephasing can only be suppressed when $\tau_D \gg \tau_B$. For $\tau_B \gtrsim \tau_D$, the Bloch vectors of the grating no longer precess around the \hat{y} -axis but rather around an axis at an angle $\theta_k(t) = \arctan(U_0 \sum_{k'} V_{k'}^{(b)}(t)/\delta\omega_k)$ relative to the \hat{z} -axis at the “generalized Rabi frequency” $\sqrt{(U_0 \sum_{k'} V_{k'}^{(b)})^2 + \delta\omega_k^2}$. This again leads to the spreading out of the Bloch vectors in the equatorial plane and hence a collapse of the density grating. This is confirmed in Fig. 6, which shows the dynamics of the populations forming (a) the grating and (b) the beam for $N_b/N_g = 1.0$ and $\tau_D/\tau_B = 1.0$. It illustrates clearly the frequency dependence on k familiar from the generalized Rabi oscillations of two-level physics.

The four-wave mixing efficiency can be quantified by the maximum number of beam atoms that can be scattered by the grating. Initially the beam atoms are scattered into negative momentum states, hence the peak efficiency is given by the first maximum of

$$\eta(t) = \sum_{|k| < k_{F,b}} n_{k-q/2}^{(b)}(t)/N_b. \quad (25)$$

Fig. 7 shows η_{max} for different dephasing times. We observe a rapid decrease in efficiency when $N_b/N_g > 1/2$. This result can be explained in terms of the Bloch vector model: we show in the appendix that when $N_b > N_g/2$, the maximum number of beam atoms that can be scattered into states around $-q/2$ is $N_g/2$. In practice, the efficiency can exceed this maximum value due to the residual coupling to states around $\pm 3q/2$, which enhances the density modulation of the grating. Fig. 7 also illustrates the dramatic reduction in efficiency caused by the dephasing of the grating. Even in that case, though, the achievable efficiencies indicate that four-wave mixing should still be observable when the Fermi gases used for the grating and the beam contain comparable numbers of atoms.

Interestingly, one can improve the efficiency significantly by choosing unequal probability amplitudes for the components of the grating, that is, by replacing the initial state $|\Psi^{(g)}\rangle$ of Eq. (5) by the more general superposition state

$$|\Psi^{(g)}\rangle = \prod_{|k| \leq k_{F,g}} \left(c_{-q/2} a_{k-q/2\uparrow}^\dagger + c_{q/2} a_{k+q/2\uparrow}^\dagger \right) |0\rangle \quad (26)$$

with $c_{-q/2} > c_{q/2}$ in our case. Fig. 8 plots the Bragg efficiency for several values of $c_{q/2}$ and $c_{-q/2}$, showing a maximum improvement of about 25% as compared to the case of equal initial amplitudes, $c_{-q/2} = c_{q/2} = 1/\sqrt{2}$. Even though $c_{q/2} = c_{-q/2} = 1/\sqrt{2}$ produces an initial density grating with the largest possible amplitude, subsequent scattering of beam atoms will reduce the size of the grating. In contrast, while the amplitude of the density grating produced by an unequal initial superposition

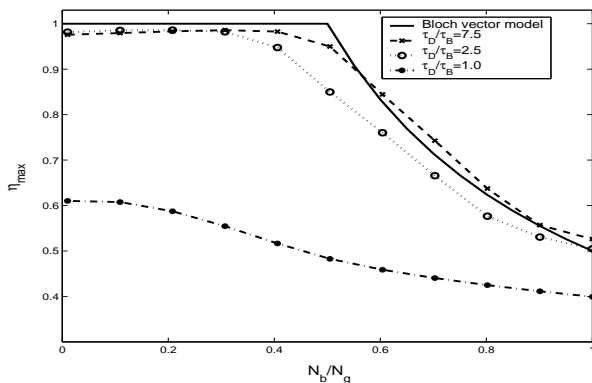


FIG. 7: Diffraction efficiency η_{max} as a function of N_b/N_g for $\tau_D/\tau_B = 7.5$ (dotted-line), 2.5 (dashed line), and 1.0 (dash-dot line), with $\omega_q/N_g U_0 = 2$. The solid line corresponds to maximum efficiency calculated from the Bloch vector model.

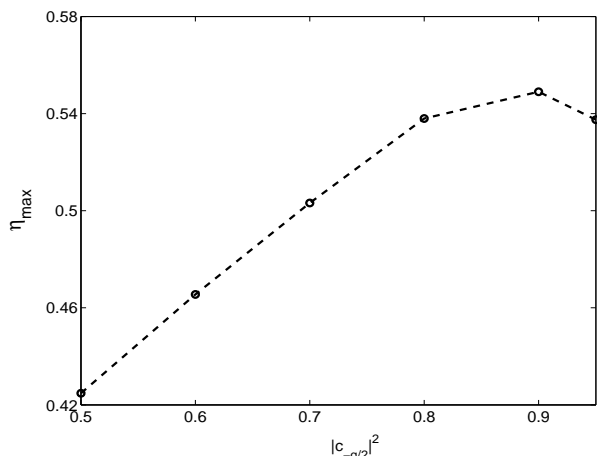


FIG. 8: η_{max} as a function of initial probability amplitudes for the grating $|c_{-q/2}|^2 = 1 - |c_{q/2}|^2$, with $\tau_D/\tau_B = 1.0$, $N_b/N_g = 0.8$.

state is less than optimal initially, the subsequent scattering of beam atoms from $|k - q/2\rangle$ to $|k + q/2\rangle$ increases $c_{q/2}$ while reducing $c_{-q/2}$, resulting in a net increase over time in the grating amplitude.

CONCLUSIONS

In this paper we have investigated purely fermionic four-wave mixing in a manner that accounts for the back-action of the scattered beam on the density grating. Our numerical results indicate that the lifetime for fermionic four-wave mixing can be dramatically improved by making the number of atoms in the beam comparable to the number of atoms that form the density grating. Although the effects of the beam on the grating does reduce the

overall efficiency of the process, the efficiencies that we have calculated indicate that it should be possible to convert in excess of 10% of the atoms in the incident beam into a fourth scattered beam.

It is well known that four-wave mixing with bosons can lead to the generation of squeezed states [24, 25]. Therefore a central feature of future work will examine the statistical properties of the scattered beam generated by the four-wave mixing to see if it is possible to generate novel fermionic states. This will involve going beyond the factorization ansatz in Eq. (9) to calculate higher order moments for the particle hole operators. Phase conjugation should also be possible if one uses a superfluid Fermi gas due to the presence of anomalous moments, $\langle a_{k\uparrow} a_{-k\downarrow} \rangle$, resulting from the formation of Cooper pairs.

This work is supported in part by the US Office of Naval Research, by the National Science Foundation, by the US Army Research Office, by the National Aeronautics and Space Administration, and by the Joint Services Optics Program. H. C. acknowledges the support of the Studienstiftung des deutschen Volkes. One of the author (T. M.) is supported by JSPS of Japan.

APPENDIX

In this appendix we solve the coupled Bloch equations for the beam and grating with $\delta\omega_k = 0$. By introducing the normalized vectors

$$u^{(b,g)} = \sum_k U_k^{(b,g)} / N_{b,g}, \quad (27)$$

$$v^{(b,g)} = \sum_k V_k^{(b,g)} / N_{b,g}, \quad (28)$$

$$w^{(b,g)} = \sum_k W_k^{(b,g)} / N_{b,g}, \quad (29)$$

we obtain the equations of motion

$$\dot{u}^{(b)} = -U_0 N_g w^{(b)} v^{(g)}, \quad (30)$$

$$\dot{v}^{(b)} = U_0 N_g w^{(b)} u^{(g)}, \quad (31)$$

$$\dot{w}^{(b)} = U_0 N_g (u^{(b)} v^{(g)} - v^{(b)} u^{(g)}), \quad (32)$$

$$\dot{u}^{(g)} = -U_0 N_b w^{(g)} v^{(b)}, \quad (33)$$

$$\dot{v}^{(g)} = U_0 N_b w^{(g)} u^{(b)}, \quad (34)$$

$$\dot{w}^{(g)} = U_0 N_b (u^{(g)} v^{(b)} - v^{(g)} u^{(b)}), \quad (35)$$

subject to the initial conditions $u^{(g)}(0) = w^{(b)}(0) = 1$. Here, the $\dot{}$ represents differentiation with respect to time. We note that the constants of motion given by (15) and (16) can be expressed as

$$N_b w^{(b)} + N_g w^{(g)} = N_b. \quad (36)$$

For our particular initial conditions we have $u^{(b)}(t) = v^{(g)}(t) = 0$ for all times. This allows us to parameterize

the solution in terms of the angles $\theta_b(t)$ and $\theta_g(t)$, of the beam and grating Bloch vectors relative to the \hat{z} -axis in the $\hat{y}\hat{z}$ - and $\hat{x}\hat{z}$ -planes, respectively,

$$w^{(b)}(t) = \cos \theta_b(t), \quad (37)$$

$$v^{(b)}(t) = \sin \theta_b(t), \quad (38)$$

$$w^{(g)}(t) = \cos \theta_g(t), \quad (39)$$

$$u^{(g)}(t) = \sin \theta_g(t). \quad (40)$$

By introducing the sum and difference angles

$$\theta_{\pm} = \theta_g \pm \theta_b - \pi,$$

we obtain the uncoupled equations

$$\ddot{\theta}_{\pm} + \omega^2 \sin \theta_{\pm} = 0, \quad (41)$$

where $\omega = U_0 \sqrt{N_g N_b}$. Eq. (41) is the equation of motion for a plane pendulum [26].

Since the initial conditions for these pendula are $\theta_{\pm}(0) = -\pi/2$ and $\dot{\theta}_{\pm}(0) = \pm N_g U_0$, a small amplitude linearization of the equations of motion is not justified. However it is still possible to find a solution. We can express the total "energy" for the pendula as

$$\frac{1}{2} \dot{\theta}_{\pm}^2 + 2\omega^2 \sin^2(\theta_{\pm}/2) = 2\omega^2 \kappa^2,$$

where

$$\kappa^2 = \frac{1}{2} + \frac{1}{4} \frac{N_g}{N_b},$$

and $\theta_{\pm,0} = 2 \arcsin \kappa$ are the turning points for the pendula. If $N_b < N_g/2$, then there are no turning points and the pendula undergo complete revolutions about "their" axes. In this case the Bloch vector for the beam undergoes complete revolutions in the $\hat{y}\hat{z}$ -plane as can be seen from Eq. (36).

If, on the other hand, $N_b > N_g/2$, then we have the oscillatory solution [27],

$$\sin(\theta_{\pm}(t)/2) = \pm \kappa \operatorname{sn}(\omega(t \mp t_0), \kappa) \quad (42)$$

where sn is a jacobian elliptic function [28] and t_0 is determined by the initial condition, $\kappa \operatorname{sn}(\omega t_0, \kappa) = 1/\sqrt{2}$. In this case the beam Bloch vector has a turning point at $\cos \theta_b = 1 - N_g/N_b$, so that the maximum number of beam atoms that can be scattered into states around $-q/2$ is $N_g/2$. The period of the oscillations for the elliptic function is given by Eq. (24).

- [2] L. Deng, E. W. Hageley, J. Wen, M. Trippenbach, Y. Band, P. S. Julienne, J. E. Simsarian, K. Helmerson, S. L. Rolston, and W. D. Phillips, *Nature* **398**, 218 (1999).
- [3] S. Innouye, T. Pfau, A. P. Chikkatur, A. Görlitz, D. E. Pritchard and W. Ketterle, *Nature* **402**, 641 (1999); M. Kozuma, Y. Suzuki, Y. Torii, T. Sugiura, T. Kuga, E. W. Hageley, and L. Deng, *Science* **286**, 2309 (1999).
- [4] S. Burger, K. Bongs, S. Dettmer, W. Ertmer, K. Senstock, A. Sanpera, G. V. Shlyapnikov, and M. Lewenstein, *Phys. Rev. Lett.* **83**, 5198 (1999).
- [5] K. E. Strecker, G. B. Partridge, A. G. Truscott, and R. G. Hulet, *Nature* **417**, 150 (2002).
- [6] J. M. Vogels, K. Xu, and W. Ketterle, *Phys. Rev. Lett.* **89**, 020401 (2002).
- [7] J. M. Vogels, J. K. Chin, and W. Ketterle, *cond-mat/0209067*.
- [8] R. Wynar, R. S. Freeland, D. J. Han, C. Ryu, and D. J. Heinzen, *Science* **287**, 1016 (2000).
- [9] C. McKenzie *et al.*, *Phys. Rev. Lett.* **88**, 120403 (2002).
- [10] A. G. Truscott, K. E. Strecker, W. I. McAlexander, G. B. Partridge, R. G. Hule, *Science* **291**, 2570 (2001); F. Schreck, G. Ferrari, K. L. Cubizolles, L. Khaykovich, M.-O. Mewes, and C. Salomon, *Phys. Rev. A* **64**, 011402 (2001).
- [11] B. DeMarco, and D. S. Jin, *Science* **285**, 1703 (1999).
- [12] Z. Hadzibabic, C. A. Stan, K. Dieckmann, S. Gupta, M. W. Zwierlein, A. Görlitz, and W. Ketterle, *Phys. Rev. Lett.* **88**, 160401 (2002).
- [13] G. Roati, F. Riboli, G. Mondugno, and M. Ingusco, *Phys. Rev. Lett.* **89**, 150403 (2002).
- [14] K. M. O'Hara, S. L. Hemmer, M. E. Gehm, S. R. Granade, and J. E. Thomas, *Science* **298**, 2179 (2002).
- [15] W. Ketterle, and S. Inouye, *Phys. Rev. Lett.* **86**, 4203 (2001).
- [16] M. G. Moore, and P. Meystre, *Phys. Rev. Lett.* **86**, 4199 (2001).
- [17] P. Villain, P. Öhberg, L. Santos, and M. Lewenstein, *Phys. Rev. A* **64**, 023606 (2001).
- [18] H. Christ, C. P. Search, and P. Meystre, *cond-mat/0212384*.
- [19] B. DeMarco, and D. S. Jin, *Phys. Rev. A* **58**, 4267 (1998).
- [20] Y. Torii *et al.*, *Phys. Rev. A* **61**, 041602 (2000).
- [21] A. G. Rojo, J. L. Cohen, and P. R. Berman, *Phys. Rev. A* **60**, 1482 (1999).
- [22] Kerson Huang, "Statistical Mechanics" (John Wiley & Sons, New York, 1987).
- [23] P. Meystre and M. Sargent, "Elements of Quantum Optics" Third Edition (Spinger-Verlag, Berlin, 1999).
- [24] H. P. Yuen and J. H. Shapiro, *Opt. Lett.* **4**, 334 (1979).
- [25] R. E. Slusher *et al.*, *Phys. Rev. Lett.* **55**, 2409 (1985).
- [26] J. B. Marion and S. T. Thornton, "Classical Dynamics of Particles and Systems, Third Edition" (Harcourt Brace Jovanovich, San Deigo, 1988).
- [27] E. T. Whittaker, "A Treatise on the Analytical Dynamics of Particles and Rigid Bodies" (Cambridge University Press, Cambridge, UK, 1927).
- [28] M. R. Spiegel, "Mathematical Handbook" (McGraw Hill, New York, 1997).

[1] G. Lenz, P. Meystre, and E. M. Wright, *Phys. Rev. Lett.* **71**, 3271 (1993).